

Dynamic spectrum assignment in multicell OFDMA networks enabling a secondary spectrum usage

Francisco Bernardo^{*,†}, Ramón Agustí, Jordi Pérez-Romero and Oriol Sallent

Department of Signal Theory and Communications, Universitat Politècnica de Catalunya, Spain

Summary

The aim of this paper is to propose a set of novel Dynamic Spectrum Assignment (DSA) algorithms for multicell Orthogonal Frequency Division Multiple Access (OFDMA) scenarios. Thanks to the proposed algorithms, licensed spectrum holders can release spectrum bands in large geographical areas to be leased to other secondary markets in a cognitive radio environment, while preserving the quality of service (QoS) of the licensed users in the system. Results are obtained comparing the proposed schemes against other conventional frequency reuse strategies, revealing significant improvements in terms of both spectral efficiency and opportunities for secondary usage. Copyright © 2009 John Wiley & Sons, Ltd.

KEY WORDS: dynamic spectrum assignment; multicell OFDMA; cognitive radio; secondary spectrum usage

1. Introduction

The regulatory perspective on how the spectrum should be allocated and utilized in future wireless scenarios is evolving toward a cautious introduction of more flexibility in spectrum management together with economic considerations on spectrum trading. This new spectrum management paradigm is driven by the growing competition for spectrum and the requirement that the spectrum is used more efficiently [1]. A broad view in that respect is to examine spectrum utilization from a time/location/band/power perspective as suggested in the Federal Communications Commission Spectrum Policy Task Force Report [2], where it was stated that the spectrum shortage results from the

spectrum management policy rather than the physical scarcity of the usable frequencies. Since then, this under utilization of spectrum has stimulated a great research interest in searching for better spectrum management policies and techniques that enable the use of the available spectrum optimally in time and space [3].

To this end, different spectrum access management models have been identified in [4,5] being currently under consideration by the spectrum regulatory bodies. Briefly, the taxonomy of dynamic spectrum access management identifies three models: (1) The *Dynamic Exclusive Use Model* allocates the spectrum bands for exclusive use of services and operators along time and space. Primary operators (i.e., the licensees

*Correspondence to: Francisco Bernardo, Universitat Politècnica de Catalunya, Jordi Girona 1-3, Campus Nord, D4-115, 08034 Barcelona, Spain.

†E-mail: fbernardo@tsc.upc.edu

of the spectrum) have the usage right of a specific band but, within this model, they agree to trade their spectrum with other spectrum licensees (of the same or different services), (2) The *Hierarchical Access Model* divides users between primary users (licensed users) and secondary opportunistic cognitive radio users. This model mainly focuses on how secondary users may use the primary spectrum without interfering primary users' communications. In this sense, secondary users fill the spatial and temporal opportunities that primary usage of the spectrum generates. Notice that in this model primary operators do not necessarily perform an advanced management of their spectrum and may be unaware of secondary users' presence. In this sense, they could be reluctant to altruistically open their expensive spectrum licenses for secondary spectrum usage—except for emergency, safety, and similar services. (3) The *Commons Model* promotes an open sharing of the spectrum even without the control of the governmental regulation bodies in some cases. This model would achieve the greatest spectrum access efficiency since any piece of the spectrum (licensed or not) would be shared spatially and temporally by primary and secondary users, in principle without any regulatory barrier. Within this new spectrum access paradigm, the so called *Private Commons* [5,6] has arisen, where primary spectrum owners agree to lease their spectrum to secondary markets in spectrum (i.e., potential opportunities of secondary usage of the spectrum) to be used in an infrastructure-less manner (e.g., opportunistic *ad hoc* cognitive radio networks). The main difference with the *Hierarchical Access Model* is that, here, primary operators are keen to open their spectrum and to generate spectrum opportunities for secondary usage, since they may charge a fee for each commercial secondary spectrum access.

This paper is focused on the Private Commons model. Within this initiative, primary operators concern themselves to perform a Dynamic Spectrum Assignment (DSA) strategy with the objective of maximizing spectral efficiency. For this purpose, primary operators attempt to guarantee the Quality of Service (QoS) of their users with the minimum spectrum whereas, on the other hand, attempt to release pieces of spectrum in large geographical areas to create spectrum access opportunities. In this sense, both primary and secondary users exploit spectrum opportunities at maximum, and thus, the primary operator obtains an additional revenue stream from spectrum trading activities with the secondary market.

According to the above framework, and when focusing on a cellular primary network, two technical requirements rise up to build this initiative:

1. A flexible Radio Access Technology (RAT) that enables the pooling of the spectrum in a group of contiguous cells. Orthogonal Frequency Division Multiple Access (OFDMA) has been seen as the candidate technology for obtaining such a flexible radio interface [7,8] since OFDMA subcarriers (or groups of contiguous subcarriers named *chunks*) can be pooled, assigned to different cells, and transmitted with different powers to generate spectral gaps in regional areas.
2. DSA techniques over the radio interface that (a) automatically adapt systems' spectrum to primary users' QoS requirements, taking into account the spatial and temporal variations of the network load, (b) mitigate intercell interference in order to increase the capacity per frequency resource (usually limited by the Signal to Interference Ratio (SIR)), and (c) pool and release pieces of spectrum in a given region.

In this work, a novel DSA framework enabling secondary cognitive radio usage in a multicell OFDMA system is presented. This is actually a multiple access technique that is in the main stream of current new proposed systems (LTE, WiMax) and at the same time is quite suitable for cognitive radio implementations [9,10]. Furthermore, to the best of the authors' knowledge this is the first technical proposal in the open literature to implement the Private Commons framework from a primary operator point of view, at least in the above mentioned OFDMA multicell environment. To this end, four DSA algorithms are presented. All of them autonomously react to network condition variations to provide a proper spectrum assignment per cell by taking advantage of the heterogeneous spatial traffic distributions. The four DSA algorithms have been compared with the fixed frequency reuse schemes so far proposed for cellular OFDMA planning, showing that the proposed schemes (1) improve spectral efficiency, (2) maintain users' QoS satisfaction, and (3) enable opportunistic spectrum access (by releasing some frequency bands in large geographical areas) in a way that secondary spectrum usage might be introduced without penalizing the primary licensed users. The proposed DSA strategies are in essence a form of *self-organized* processes, [11] since it is intended that they are executed with minimum human interaction. Thus,

operational costs can be reduced while adaptability and robustness is given to the network since DSA strategies autonomously maintain the service level and spectral efficiency when facing network changes or failures.

The remaining of the paper is organized as follows: a discussion about the DSA framework and system model is carried out in Section 2. Before entering into the details of the proposed DSA algorithms, a review of the current spectrum management schemes for OFDMA is presented in Section 3. The DSA algorithms proposed in this paper are explained in detail in Section 4. Section 5 is devoted to the simulation model, whereas results obtained are exposed in Section 6. Finally, Section 7 summarizes the conclusions.

2. DSA Framework

This section is devoted to explain the proposed system model or DSA framework. Figure 1(a) illustrates a primary operator that coexists in a given geographical region with a potential secondary market. Thanks to DSA operation, the primary operator may share its licensed spectrum bands with the secondary market whose users are granted to opportunistically access the released pieces of the spectrum. The spatial distribution of the primary traffic may be different within the operation area. Figure 1(a) shows an example of how two subareas could be differentiated; one residential subarea and a business subarea. Traffic distribution in these subareas might be different depending on the hour of the day. Therefore, traffic distribution affects primary usage of spectrum temporally and spatially

in the long-term (i.e., hours). As a result, the DSA operation tries to adjust the primary spectrum to these variations and thus to generate spectrum opportunities for secondary market in the less loaded areas.

The *Commons* paradigm states that spectrum access or management does not need government/private regulation [5]. However, it has been stated that some kind of coordination between the primary owner of the spectrum license and the secondary market is needed [12]. Then a *secondary spectrum coordination entity* that manages the spectrum transactions between primary and secondary markets could become necessary, although it is out of the scope of this paper.

Figure 1(b) illustrates a hierarchical architecture within the primary operator who deploys a multicell cellular system with an OFDMA-based radio interface. The *DSA controller* provides the cell-by-cell DSA in the system in the long-term. On the other hand, the *Short-Term Scheduler (STS)* tries to exploit multiuser diversity due to fast frequency dependant fading in the short-term, and is in charge of scheduling users' transmissions by using the available spectrum in each cell. Similar dual architectures have also been reported in 3GPP [13] or in recent related work [7,14]. Next subsection details the OFDMA system model adopted, whereas more details about the STS and the DSA controller are given in Sections 2.2 and 2.3 respectively.

2.1. OFDMA System Model

DSA is considered for the downlink of an OFDMA-based radio interface. Typically, the radio resources in

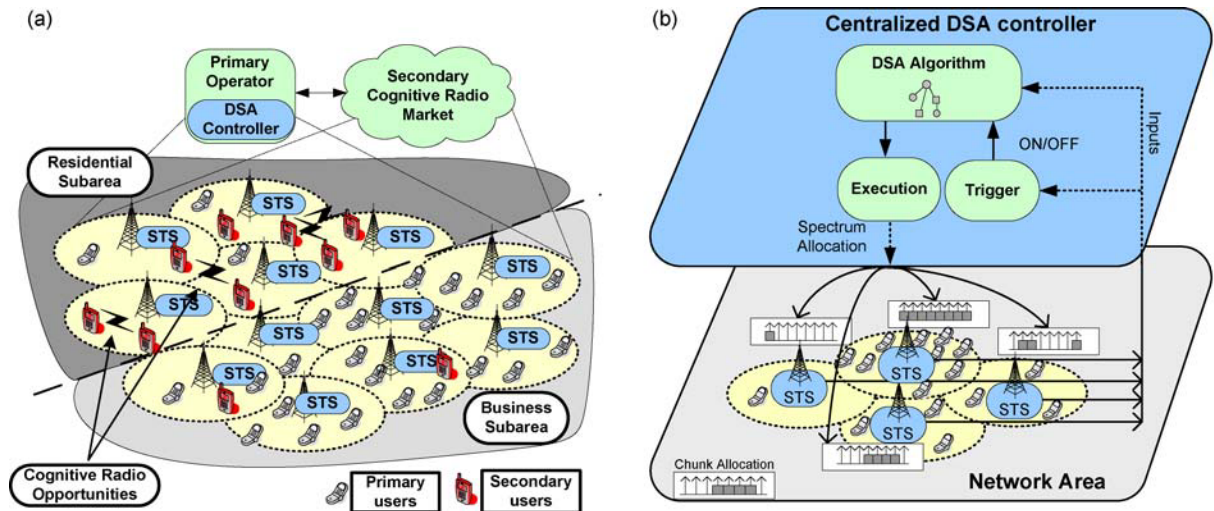


Fig. 1. (a) DSA framework architecture and (b) Centralized DSA controller.

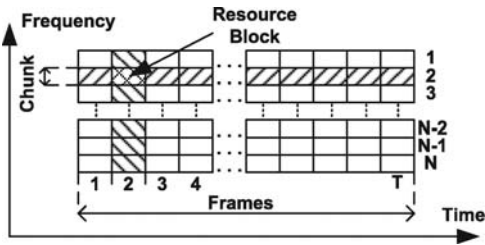


Fig. 2. Generic time–frequency grid in OFDMA radio access networks.

OFDMA RATs are divided in both time and frequency building a time–frequency grid (Figure 2) where the minimum radio resource that can be assigned to a user is usually named as a *Resource Block* (RB). In frequency, the whole available band is divided into groups of adjacent subcarriers or *chunks*, whereas in time it is divided into frames. Therefore, this RAT is flexible enough to be exploited by a DSA strategy.

The Signal to Interference plus Noise (SINR) ratio is calculated per each chunk as

$$\gamma_{m,n} = \frac{P_i G_{i,m} S_{i,m} F_{i,m,n}}{\sum_{\substack{j \in \Phi_n \\ j \neq i}} (P_j G_{j,m} S_{j,m} F_{j,m,n}) + P_{\text{noise}}} \quad (1)$$

where $\gamma_{m,n}$ represents the SINR in the n th chunk for the m th user, index i represents the serving cell and j any interfering cell taken from the set of cells using the n th chunk (denoted as Φ_n). P_i stands for the transmitted chunk power including transmitter and receiver antenna gains. Path loss and large scale fading is considered flat for all the chunks while fast frequency selective fading may vary from one chunk to another depending on users' speed. $G_{i,m}$ denotes the distance dependant channel gain (inverse of path loss), $S_{i,m}$ the large scale fading (shadowing), and $F_{i,m,n}$ the fast frequency selective fading component that depends on the chunk n . Finally, P_{noise} denotes the total thermal noise power. Users' transmission bit rate is variable by means of Adaptive Coding and Modulation (ACM). The achievable user bit rate considered is computed for each chunk as [15]

$$R_{m,n} = \frac{W}{N} \log_2 \left(1 - \frac{1.5\gamma_{m,n}}{\ln(5\text{BER})} \right) = \frac{W}{N} q_{m,n} \quad (2)$$

where $R_{m,n}$ is the m th user's bit rate, W/N is the chunk bandwidth and BER stands for the Bit Error Rate. It is also supposed that perfect channel state information

is available at both the transmitter and receiver sides. Notice that $R_{m,n}$ depends on the available spectral efficiency $q_{m,n}$, which in this work will be limited to a maximum value of $\eta_{\text{max}} = 4$ bits/s/Hz corresponding to 64 QAM with a coding rate of 2/3.

2.2. Short-Term Scheduler

Following the current trend of decentralizing functions toward edge network nodes, which enables shorter frame durations, lower latencies, and higher speed channels, the STS is located at the base station, e.g., the eNB (E-UTRAN NodeB) in the particular case of the architecture proposed for Long-Term Evolution (LTE) by 3GPP in Reference [13].

The STS schedules the radio transmissions of users served by a given cell in the time–frequency grid, by deciding which RBs are allocated to each user. Notice that due to DSA, a cell may not have all the chunks available, and thus, the STS schedules transmissions only in the available RB.

Different policies could be followed by the STS for scheduling users. For example, they may be scheduled as a function of channel quality, buffer delay, throughput, buffer occupancy, service, etc. In any case, the STS is traffic- and channel-aware in its decisions, and tries to exploit frame by frame the multiuser diversity by using the available resources at each cell. In this work, a Generalized Proportional Fair (GPF) algorithm has been used since this scheme provides a good trade-off between fairness and throughput and exploits multiuser diversity in both time and frequency [16].

2.3. DSA Controller

In this paper, the DSA operation of a single primary operator is studied (Figure 1(b)). The DSA controller is located in a network node with the ability to control a set of cells. The objective of this mechanism is to automatically adapt the system's spectrum to traffic variations in time and space in the long-term while maintaining users' satisfaction and avoiding intercell interference. Furthermore, it should attempt to achieve an efficient spectrum usage by releasing unnecessary frequency resources that can be used by secondary cognitive radio users. Hence, the DSA controller implements the mechanisms to perform a self-organized DSA.

To decide the chunks assigned to each cell the DSA controller executes the DSA algorithms that are explained in Section 4. The following inputs, triggers, and outputs of this module are identified:

- **Inputs:** Inputs for the DSA controller come from each cell under its control and include the number of users per cell, the deployment of cells, the powers devoted per chunk, and some QoS indicators. In this work, as a QoS metric the dissatisfaction probability $P^{T_{th}}$ is defined as the probability that the average throughput of the users in the system during last second is lower than a threshold T_{th} , called the satisfaction throughput. A formal definition of $P^{T_{th}}$ is given in Section 6.
- **Triggers:** The DSA algorithm could be triggered either periodically in relatively long-term periods (e.g., in the order of tenths of minutes given the slow traffic variation envisaged) or each time the dissatisfaction probability $P^{T_{th}}$ rises above a given threshold.
- **Outputs:** The main output of the DSA controller is the specific assignment of chunks to each cell. Different cells are given different number of chunks depending on their traffic status. Furthermore, the location of the chunks within the system's band is also taken into account in order to mitigate the intercell interference and increase the number of non-assigned chunks to a cluster of cells. The decision maker takes the outcome of the DSA algorithm and enforces the actual new spectrum assignment.

3. Fixed Frequency Reuse and Interference Management

Prior to presenting the DSA algorithms, a discussion about the conventional frequency reuse schemes existing in the literature is given in this section. In an OFDMA RAT, intracell interference is usually avoided by means of scheduling mechanisms that only allow an RB to be assigned to a single user within a given cell at a given time. On the other hand, due to spatial and temporal traffic variations and the lack of coordination between the traffic schedulers in different cells, intercell interference cannot be easily avoided with scheduling mechanisms. Hence, in order to combat the intercell interference, different Frequency Reuse Factors (FRF) that distribute the total spectrum band of the system over different cells have been proposed. These FRF are deployed in the network off-line within the planning phase.

Figure 3(a) represents the FRF schemes studied in this section depending on the system's band division and the power assigned per subband. The simplest FRF scheme is $FRF = 1$ where all chunks are available at any cell and are transmitted with the same power (denoted in the following as FRF1). In this scheme, the users at the edge of the cell experience high interference because all neighboring cells reuse the same frequency. A possibility to mitigate this interference for these users is to increase the reuse factor. Applying a $FRF = M > 1$ implies that the total band is divided into M equal subbands, and

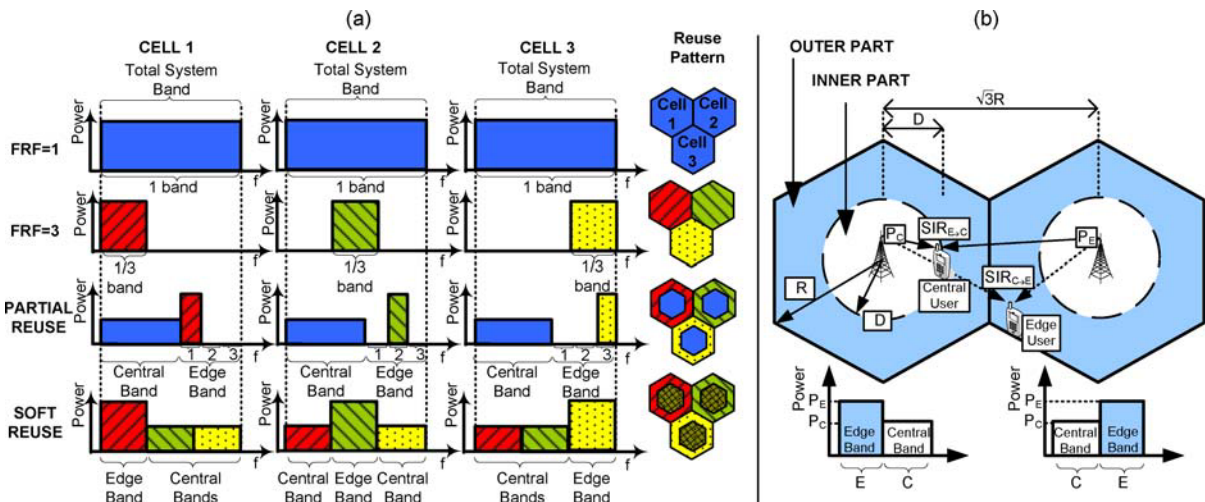


Fig. 3. (a) Fixed frequency reuse schemes considered in this paper, (b) cellular deployment for soft reuse and partial reuse schemes.

is distributed over groups of M contiguous cells (or clusters) repeating this pattern in the cellular system. As in the FRF1, all the chunks are transmitted with the same power. This scheme reduces the intercell interference but reduces by M the cell potential capacity as well. Figure 3(a) represents this scheme when M takes a value equal to 3 (denoted as FRF3 hereafter).

There are also other reuse schemes recently proposed [17,18] that are based on the division of the frequency band, the users, and the cells between the central (inner) and edge (outer) sets. Figure 3(b) depicts an example of the cellular deployment for these schemes. Users within a cell are classified between central or edge users depending on whether they are located in the inner or outer part of the cell respectively. C chunks are reserved for the central subband and E chunks for the edge subband. Central chunks are transmitted with power P_C and edge chunks with power P_E ($P_C \leq P_E$). Therefore, due to coverage reasons, central chunks are for exclusive usage of central users, whereas edge users have priority to use the edge chunks. Nevertheless, central users may be granted with the edge chunks if edge users' transmissions are not scheduled in them. Notice that the worst SIR (denoted as $SIR_{E \rightarrow C}$) for central users in a cell is given when the assigned chunks for central usage in this cell are the same as those devoted to edge usage in neighboring cells. However, in the same conditions edge users increment their SIR ($SIR_{E \rightarrow C}$) because neighboring cells transmit with power $P_C \leq P_E$. Then careful setting of these powers should be performed as it is explained in Section 5.

Partial frequency Reuse (PR) [17] divides the total band of the system between a central and an edge subband (Figure 3(a)). The central subband is available in all cells (FRF1), whereas the edge subband is further divided in three equal subsets that are distributed regularly (FRF3) over cells. In this case $C + E/3$ chunks are assigned per cell.

Soft-frequency Reuse (SR) Scheme [18] divides the frequency band into three subbands, all of them available in all the cells (Figure 3(a)). However, the edge subband, serving the edge users, is transmitted with greater power than the other two central subbands that are only available for the central users. As in the $FRF = 1$ scheme, all cells have all chunks available, but those belonging to the edge subband alternate their position into the system's band following a FRF3 scheme. The total number of chunks in each cell is $C + E$ chunks.

4. Dynamic Spectrum Assignment Algorithms

The above summarized FRF schemes deploy a fixed reuse pattern over the network that limits the system's performance. These strategies are static and inflexible since the assignment of the frequency resources to cells is homogeneous and cannot be changed online. This implies that the frequency deployment may not be adapted to heterogeneous spatial traffic distributions and their variation in time. Moreover, it is difficult to find a group of cells where the same spectrum band is not used, what prevents them from being offered to a spectrum secondary market.

In this paper, a set of DSA algorithms is proposed to dynamically adjust the spectrum to temporal and spatial variations of the load. These algorithms are self-adaptive in the sense that they learn from experience how to better adapt to the network conditions. Therefore, to avoid wasting frequency resources and to generate spectrum pools for secondary usage, different cells are given different number of chunks depending on their traffic load, channel conditions, and users' QoS requirements.

Four DSA algorithms named DSA1, DSA2, DSA3, and DSA4 are introduced to cope with the limitations of the fixed FRFs. These algorithms are executed in two steps. First, the number of chunks to be assigned to each cell considering the cell load and users' QoS requirements is computed and, afterwards, an assignment procedure that mitigates intercell interference (cost of assignment) is executed to decide the specific chunks to be assigned per cell. That is, the objective of any of the DSA algorithms is to build an assignment set $\Upsilon = \{\Psi_1, \Psi_2, \dots, \Psi_K\}$ where Ψ_j is the set of chunks assigned to cell j . The high level description of the procedure executed by the algorithms is schematically represented in Figure 4.

DSA1 and DSA2 algorithms follow the same deployment as FRF1 and FRF3 respectively (i.e., the same power is devoted to all chunks and there is no division between central and edge sets, neither in the spectrum nor in the cell and users). The DSA1 algorithm estimates the number of chunks per cell based on the number of users per cell and their throughput requirements. However, the DSA1 algorithm considers a fixed chunk capacity to estimate the number of chunks needed. In consequence, it may not properly adapt the number of chunks per cell if the real average capacity per chunk differs from the original estimation. The DSA2 algorithm self-tunes its

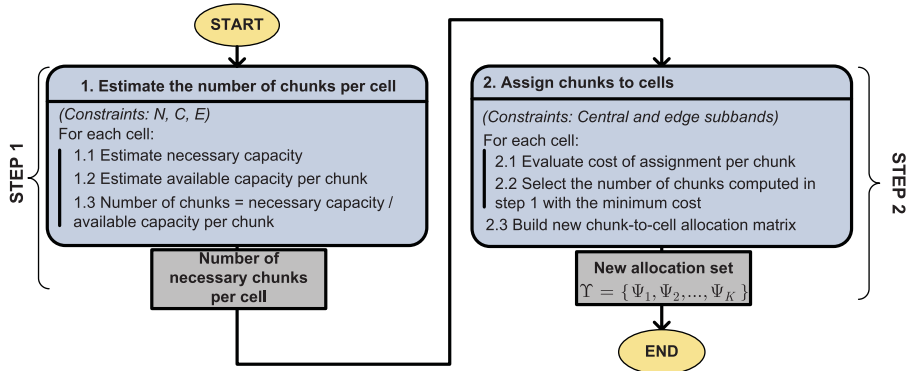


Fig. 4. High level description of the DSA algorithms.

parameters to better adjust to the real average capacity per chunk and consequently better adapts the number of chunks to the cells' requirements. Both algorithms execute the same chunk–cell assignment procedure (step 2) that is based on minimizing the cost assignment per chunk and cell.

DSA3 and DSA4 follow the same approach as PR and SR by dividing the spectrum, cells, and users between central and edge sets. Also the power per chunk depends on its usage (i.e., the power devoted to edge usage is greater than that of the central usage). The key of this implementation is to protect the users at the edge of the cell, providing them a better SINR. As the DSA2 algorithm, the DSA3 and DSA4 algorithms also implement a self-tuning mechanism.

Following subsections are devoted to describe the implementation details for each one of the dynamic algorithms.

4.1. DSA1 Algorithm

The DSA1 algorithm was schematically introduced in Reference [19]. A more detailed description of the algorithm is given here.

Step 1: *Compute the number of chunks to be assigned in each cell.* The number of chunks is adapted to cells load (i.e., number of users) so that highly loaded cells get a high number of chunks. Specifically, given a maximum number of chunks N available in the system, the number of chunks $N_j \in \{1, 2, \dots, N\}$ assigned to the j th cell is given by

$$N_j = \min \left(N, \max \left(1, \left\lceil \frac{U_j T_{\text{th}}}{\kappa} \right\rceil \right) \right) \quad (3)$$

where $\lceil x \rceil$ denotes the nearest integer greater than or equal to x and U_j are the users served by the j th cell. T_{th} represents the satisfaction throughput per user (i.e., the minimum throughput that a user expects to be satisfied with the requested service), and κ is the estimated chunk capacity, which is assumed to be constant for DSA1 algorithm. In fact, κ could be written as $\kappa = (W/N)(\eta_{\text{max}}/f)$ in bits/s where W is the total system bandwidth (and correspondingly W/N is the chunk bandwidth), η_{max} stands for the maximum theoretical spectral efficiency due to ACM in bits/s/Hz, and $f > 1$ is an empirical *margin factor*. It is expected that due to poor channel conditions (especially for users at the edge of the cell) the average spectral efficiency obtained in the cell is lower than η_{max} . Then the margin factor reduces η_{max} in order to obtain a closer value to the actual chunk capacity. For DSA1 f is fixed and configured offline. Hence, the chunk capacity might be over- or under-estimated depending on the value of f .

Step 2: *Assign the chunks devoted to each cell determining the potential intercell interference.* The DSA1 algorithm takes into account the cell deployment and the load of the cells. That is, in order to reduce the intercell interference, the chunk assignment is performed trying to avoid that the neighboring cells use the same chunk. Also, if one cell is highly loaded, cells around it should not reuse the same chunks since this cell possibly would generate interference all the time. Alternatively, if a cell is low loaded then cells around it should avoid using the few chunks assigned to that cell, since it may not benefit from frequency diversity and therefore the interference effects may be worse. To take this into account, a symmetric $K \times K$ matrix \mathbf{A} is built (K is the number of cells), where $\mathbf{A}(i,j)$ indicates the neighboring relationship between cells i and j in

terms of loads and path losses as in the following:

$$A(i, j) = \begin{cases} 0, & \text{if } i = j \\ \left(\frac{U_i}{U_j} + \frac{U_j}{U_i} \right) \left(\frac{R}{L_{ij}} \right)^\delta, & \text{otherwise} \end{cases} \quad (4)$$

where U_j stands for the load of cell j in users, R denotes the cell radius, L_{ij} is the minimum distance from center of cell i to the border of cell j and δ is the path loss propagation exponent. Hence, matrix A is a coupling matrix based on the path losses between cells and includes the sum of load ratios in order to obtain a symmetric matrix. Notice that the term $(U_i/U_j + U_j/U_i)$ takes its minimum value when the involved cells have the same load. Then it is tried that cells with similar loads reuse the same chunk. Additionally, as the interfering cell is farther from the serving cell the cost between those cells decreases.

Therefore, the assignment procedure assigns to a given cell j the necessary chunks (N_j from the step 1) with the minimum cost. The cost of assigning the n th chunk to cell j is calculated as $\vartheta_j^{(n)} = \sum_{i \in \Phi_n} A(i, j)$ where Φ_n is the set of cells with the n th chunk assigned. A detailed description of the DSA1 algorithm is included in Table I.

4.2. DSA2 Algorithm

Unlike the DSA1 algorithm, where the margin factor f remains constant, the DSA2 algorithm adjusts the margin factor per cell f_j according to the dissatisfaction probability on the cell ($P_j^{T_{th}}$). Thus, it provides a better estimation of the capacity per chunk $\kappa_j = (W/N)(\eta_{max}/f_j)$ than DSA1. The margin factor f_j is updated as

$$f_j = \begin{cases} f_j - \Delta f, & \text{if } P_j^{T_{th}} \leq P_{low} \\ f_j, & \text{if } P_{low} \leq P_j^{T_{th}} \leq P_{up} \\ f_j + \Delta f, & \text{if } P_j^{T_{th}} \geq P_{up} \end{cases} \quad (5)$$

where Δf_j is defined as the *margin factor step*, $P_j^{T_{th}}$ is the average dissatisfaction probability for cell j , and P_{low} and P_{up} are the dissatisfaction probability thresholds to decrease and increase the margin factor respectively.

Step 1: Compute the number of chunks to assign in each cell. After updating the margin factor using Equation (5), the number of chunks to be assigned to the cell j is then computed using Equation (3) after substituting κ by $\kappa_j = (W/N)(\eta_{max}/f_j)$. Notice

that the DSA2 tends to maintain the dissatisfaction probability between P_{low} and P_{up} if possible, which reduces the number of chunks used per cell if dissatisfaction probability is below P_{low} . This behavior improves the spectral efficiency and increases the number of free resources for secondary cognitive radio usage.

Step 2: Assign the chunks devoted to each cell determining the potential intercell interference. The DSA2 algorithm implements the same assignment procedure as DSA1 (Table I).

4.3. DSA3 Algorithm

Similar to the PR strategy, the DSA3 algorithm considers that the system's band is divided into two separate bands with available chunks devoted to central and edge usage respectively. The maximum number of chunks per subband is C and E for the central and the edge subbands respectively so that $N = C + E$. This division is configured by the network operator and remains the same for all the cells so that central chunks never perceive interference from an edge chunk and *vice versa*. The way this division is performed is explained in Section 5.

The DSA3 algorithm (a) computes the number of chunks needed per subband and per cell (step 1) and (b) performs the chunk-cell assignment independently per subband (step 2). As in the PR strategy, no intercell mitigation is performed for the central subband, whereas for the edge subband the same assignment strategy as in DSA1 and DSA2 algorithms is executed. Thus, DSA3 is a dynamic version of PR.

Step 1: Compute the number of chunks to assign in each cell. DSA3 algorithm computes the number of chunks to be assigned to the central band C_j and the edge band E_j for the j th cell as

$$C_j = \min \left(C, \max \left(1, \left\lceil \frac{U_{C_j} T_{th}}{(W/N) (\eta_{max}/f_j)} \right\rceil \right) \right) \quad (6)$$

$$E_j = \min \left(E, \max \left(1, \left\lceil \frac{U_{E_j} T_{th}}{(W/N) (\eta_{max}/f_j)} \right\rceil \right) \right) \quad (7)$$

where U_{C_j} and U_{E_j} are the number of users located in the central and edge part of the j th cell respectively and

Table I. DSA algorithms pseudo-codes (STEP 2)

Definitions		
K : number of cells considered. N : number of chunks available. N_j : number of chunks to assign to cell j C : maximum number of chunks in central subband C_j : number of central chunks to assign to cell j E : maximum number of chunks in edge subband E_j : number of edge chunks to assign to cell j $j \in \{1, 2, \dots, K\}$: cell index.	$n \in \{1, 2, \dots, N\}$: chunk index. $\Upsilon = \{\Psi_1, \Psi_2, \dots, \Psi_K\}$: Objective Assignment set. Ψ_j : set of chunks assigned to cell j . Φ_n : set of cells with chunk n assigned. $\Phi_n^{(E)}$: set of cells with chunk n assigned for edge usage. $\mathcal{G}_j^{(n)}$: cost of assigning chunk n to cell j . $\mathbf{A}(i, j)$: cost relationship between cells i and j (4).	
DSA1 and DSA 2	DSA3	DSA4
1: Init- $\Phi_n = \emptyset \quad \forall n$, $\Psi_j = \emptyset \quad \forall j$, $\mathcal{G}_j^{(n)} = 0 \quad \forall n, j$ 2: for all j, do Compute costs: 3: if $\exists \Phi_n \neq \emptyset$, then 4: for all n, do $\mathcal{G}_j^{(n)} = \sum_{i \in \Phi_n} \mathbf{A}(i, j)$ 5: end for 6: end if Perform assignment: 7: while $\Psi_j < N_j$, do $n^* = \arg \min_{\forall n} \{\mathcal{G}_j^{(n)}\}$ $\Psi_j \leftarrow \Psi_j \cup \{n^*\}$ $\Phi_{n^*} \leftarrow \Phi_{n^*} \cup \{j\}$ $\mathcal{G}_j^{(n^*)} = \infty$ 8: end while 9: Update Assignment set: $\Upsilon = \{\Psi_1, \Psi_2, \dots, \Psi_K\}$ 10: end for	1: Init- $\Phi_n^{(c)} = \emptyset \quad \forall n$, $\Psi_j = \emptyset \quad \forall j$, $\mathcal{G}_j^{(n)} = 0 \quad \forall n, j$ 2: for all j, do Reuse 1 for central subband: 3: $n \leftarrow 1$ 4: while $n \leq C_j$, do $\Psi_j \leftarrow \Psi_j \cup \{n\}$ $n \leftarrow n + 1$ 5: end while Compute cost edge subband: 6: if $\exists \Phi_n^{(E)} \neq \emptyset$, then 7: for all $n > C$, do $\mathcal{G}_j^{(n)} = \sum_{i \in \Phi_n^{(E)}} \mathbf{A}(i, j)$ 8: end for 9: end if Assignment edge subband: 10: while $\Psi_j < C_j + E_j$, do $n^* = \arg \min_{\forall n > C} \{\mathcal{G}_j^{(n)}\}$ $\Psi_j \leftarrow \Psi_j \cup \{n^*\}$ $\Phi_{n^*}^{(E)} \leftarrow \Phi_{n^*}^{(E)} \cup \{j\}$ $\mathcal{G}_j^{(n^*)} = \infty$ 11: end while 12: Update Assignment set: $\Upsilon = \{\Psi_1, \Psi_2, \dots, \Psi_K\}$ 13: end for	1: Init- $\Phi_n^{(c)} = \emptyset \quad \forall n$, $\Psi_j = \emptyset \quad \forall j$, $\mathcal{G}_j^{(n)} = 0 \quad \forall n, j$ 2: for all j, do Compute cost edge subband: 3: if $\exists \Phi_n^{(E)} \neq \emptyset$, then 4: for all n, do Add cost if n is for edge $\mathcal{G}_j^{(n)} = \sum_{i \in \Phi_n^{(E)}} \mathbf{A}(i, j)$ 5: end for 6: end if Assignment edge subband: 7: while $\Psi_j < E_j$, do $n^* = \arg \min_{\forall n} \{\mathcal{G}_j^{(n)}\}$ $\Psi_j \leftarrow \Psi_j \cup \{n^*\}$ $\Phi_{n^*}^{(E)} \leftarrow \Phi_{n^*}^{(E)} \cup \{j\}$ $\mathcal{G}_j^{(n^*)} = \infty$ 8: end while Compute cost central subband: 9: for all n, do 10: if $\Psi_j \cap \{n\} = \emptyset$, then Add cost if n is for edge and is not used in this cell $\mathcal{G}_j^{(n)} = \sum_{i \in \Phi_n^{(c)}} \mathbf{A}(i, j)$ 11: end if 12: end for 13: while $\Psi_j < C_j + E_j$, do $n^* = \arg \min_{\forall n} \{\mathcal{G}_j^{(n)}\}$ $\Psi_j \leftarrow \Psi_j \cup \{n^*\}$ $\mathcal{G}_j^{(n^*)} = \infty$ 14: end while 15: Update Assignment set: $\Upsilon = \{\Psi_1, \Psi_2, \dots, \Psi_K\}$ 16: end for

the margin factor per cell f_j is updated using Equation (5). Notice that the number of chunks per subband is restricted to the same C and E for any cell what could be a limitation if the cells have different loads. On the other hand, this process eases the intercell interference mitigation process, especially for edge chunks as is explained next.

Step 2: Assign the chunks devoted to each cell determining the potential intercell interference. The assignment algorithm is independently executed for each subband. Chunks devoted to the central subband are assigned to a particular cell without performing intercell interference considerations since the devoted power for those chunks has been reduced, causing then less intercell interference. Then, in this step, central chunks are consecutively assigned to a cell from the beginning of the central subband. On the other hand, the same assignment procedure as in DSA1 and DSA2 algorithms is executed for the edge subband. Therefore, the DSA3 algorithm conserves the same assignment policy as PR but applying a DSA in the edge subband. The assignment method of the DSA3 algorithm is detailed in Table I.

4.4. DSA4 Algorithm

The DSA4 algorithm goes one step further and automatically adapts the number of chunks dedicated in each cell to the central and edge subbands without the operator's intervention. It also makes a division between the central and edge chunks, adapting their number to the central and edge users' requirements respectively (step 1). Next, as in the SR scheme, the DSA4 approach permits to assign the central and edge chunks at any place within the system's band. Thus, the chunk assignment for each subband is not restricted to a specific area of the spectrum and, for example, a chunk could be assigned for edge usage in a cell even if the same chunk is reserved for central usage in other cells. DSA4 constitutes a dynamic version of SR.

Step 1: Compute the number of chunks to be assigned in each cell. The DSA4 algorithm computes the number of chunks to be assigned to the central band C_j and the edge band E_j for the j th cell as

$$C_j = \max \left(1, \left\lceil \frac{U_{C_j} T_{th}}{(W/N) (\eta_{max}/f_j)} \right\rceil \right) \quad (8)$$

$$E_j = \max \left(1, \left\lceil \frac{U_{E_j} T_{th}}{(W/N) (\eta_{max}/f_j)} \right\rceil \right) \quad (9)$$

where the total number of chunks in the cell is $N_j = C_j + E_j$. In case that the resulting number of chunks N_j is greater than the maximum available chunks N a further adjustment is carried out. Specifically, $C_j \leftarrow \lfloor N \frac{C_j}{N_j} \rfloor$ and $E_j \leftarrow \lfloor N \frac{E_j}{N_j} \rfloor$, where $\lfloor x \rfloor$ denotes the nearest integer to x . If still $N_j \neq N$ then one chunk is added to the subband with fewer chunks or subtracted from the subband with more chunks depending on whether $N_j < N$ or $N_j > N$ respectively.

Step 2: Assign the chunks devoted to each cell determining the potential intercell interference. As in the SR scheme, the DSA4 approach permits to assign the chunks for the central and edge subbands at any place within the system's band. In any case, the algorithm tries, on the one hand, to assign the best chunks for edge usage and, on the other hand, to minimize the interference generated in chunks assigned for edge usage in previous cells. First, the edge chunks are assigned in order to assure the best combination to the edge subband and next, the central chunks are assigned. In both cases, the cost $\vartheta_j^{(n)}$ of assigning the n th chunk to cell j is estimated as $\vartheta_j^{(n)} = \sum_{i \in \Phi_n^{(E)}} A(i, j)$ where $\Phi_n^{(E)}$ is the set of cells with chunk n assigned for edge usage. Notice that assigning a specific chunk n when is reserved in the neighboring cells for central usage has no cost. The reason for that is that if the chunk n is going to be used for central usage in two cells, then the reduced radius of the inner cell assures intercell interference protection for central users. On the other hand, if the chunk n is going to be used for edge usage in one cell and for central usage in the other cell then the assignment does not constitute a risk if a cautious setting of the powers devoted to the central and edge chunks is done as it is explained in the next section. Finally, the assignment procedure for the DSA4 algorithm is described in Table I as well.

5. Simulation Model

Results for a downlink multicell scenario are obtained by means of dynamic simulations. The cellular scenario is composed of $K=19$ omnidirectional cells. The maximum number of chunks in the system is $N=12$ that is big enough to provide the frequency diversity. Hexagonal cells of radius $R=0.5$ km are employed. Users are uniformly distributed within a cell and their mobility is restricted to the cell where they belong to, in order to maintain the load ratio between the cells (i.e., no handover effects are modeled). Table II

Table II. Simulation parameters.

Number of cells	$K = 19$
Cell radius	$R = 500$ m
Number of antennas	1 Tx, 1 Rx
Antenna patterns	Omnidirectional
Maximum power per chunk	$P_{\max} = 33$ dBm
Carrier frequency	2 GHz
Total bandwidth	$W = 3.75$ MHz
Number of chunks	$N = 12$
Subcarriers per chunk	25
Chunk bandwidth	$W/N = 375$ kHz
Path loss at d km [dB]	$128.1 + 37.6 \log_{10}(d)$
Path loss exponent	$\delta = 3.76$
Shadowing	Lognormal
Standard deviation	$\sigma = 8$ dB
De-correlation model	[13]
De-correlation distance	50 m
Small scale fading model	[13] TU 6-ray
UE thermal noise	-174 dBm/Hz
UE noise factor	9 dB
UE speed	3 km/h
Satisfaction throughput	$T_{th} = 128$ kbits/s
Maximum spectral efficiency	$\eta_{\max} = 4$ bits/s/Hz
BER	10^{-3}
Frame duration	2 ms
Scheduling	Proportional Fair
Averaging Window size	$T_w = 50$ frames
Initial margin factor	$f = 2.5$
Margin factor step	$\Delta f = 0.05$
Dissatisfaction probability (lower threshold)	$P_{\text{low}} = 0.1\%$
Dissatisfaction probability (upper threshold)	$P_{\text{up}} = 5\%$
DSA execution period	30 min

collects the main simulation parameters in including common configuration parameters for the DSA algorithms.

The maximum power per chunk is $P_{\max} = 32.21$ dBm (i.e., the maximum power per cell is $N \times P_{\max} = 43$ dBm) which assures the proper coverage levels at the maximum cell radius. For the PR, SR, and DSA3 algorithms careful setting of the inner zone radius and the power per chunk is also performed as is explained hereafter. Assuming that the users are uniformly distributed within a cell

under high system's load, the inner zone radius D is set so that the percentage of the total cell area devoted to the inner part equals the percentage of cell chunks ρ for that part (i.e., for Partial Reuse and DSA3 $\rho = C / (C + (E/3))$, and for Soft Reuse $\rho = C / (C + E)$). The power per edge chunk P_E is $P_E = P_{\max}$ to assure coverage in the whole cell. The power of each central chunk P_C is adjusted in order to assure that average SIR experienced by a central user located at a distance D from the center of the cell is above a protection target γ_0 whenever the worst interfering cell is using the same chunk for edge usage (see $SIR_{E \rightarrow C}$ in Figure 3(b)). Table III contains the configuration values for the PR, SR, DSA3, and also DSA4 algorithms. Since the chunk assignment policy of DSA3 algorithm is analogous to the PR scheme, for comparison purposes the maximum number of chunks devoted to each subband in both algorithms is the same. Also, DSA4 is configured to have the same inner cell radius as the SR scheme so that they are comparable.

The STS employed is a GPF scheduler [16]. Only one user is scheduled per chunk in each frame although a user could get more than one chunk per frame. Users are deployed in the scenario with their buffers always full and all the users request a satisfaction throughput $T_{th} = 128$ Kbps. This means that a user always has the information to transmit and then, he/she aims to get as much capacity as possible above 128 Kbps. If available, edge users' transmissions have priority over edge chunks. Then the scenarios are under the worst traffic load given a number of users in the scenario, which is equal to 300 active users in all the tests performed.

Four spatial distributions of the load were simulated (Figure 5). These patterns try to reflect a temporal evolution of the load in the scenario that progressively concentrates on a single cell. Thus, Figure 5(a) depicts a homogeneous distribution and Figure 5(d) a highly heterogeneous distribution, where Figure 5(b)

Table III. Configuration values for partial reuse (PR), soft reuse (SR), DSA3 and DSA4 schemes.

	Number of chunks for central usage	Number of chunks for edge usage	Central resource ratio	Inner cell radius	Protection SIR	Maximum power per edge chunk	Maximum power per central chunk
	C	E	ρ	D [m]	γ_0 [dB]	P_E [dBm]	P_C [dBm]
PR	3	9	0.5	321.52	3	32.21	26.63
SR	8	4	0.67	371.26	3	32.21	31.33
DSA3	3	9	0.5	321.52	3	32.21	26.63
DSA4	N/A	N/A	N/A	371.26	3	32.21	31.33

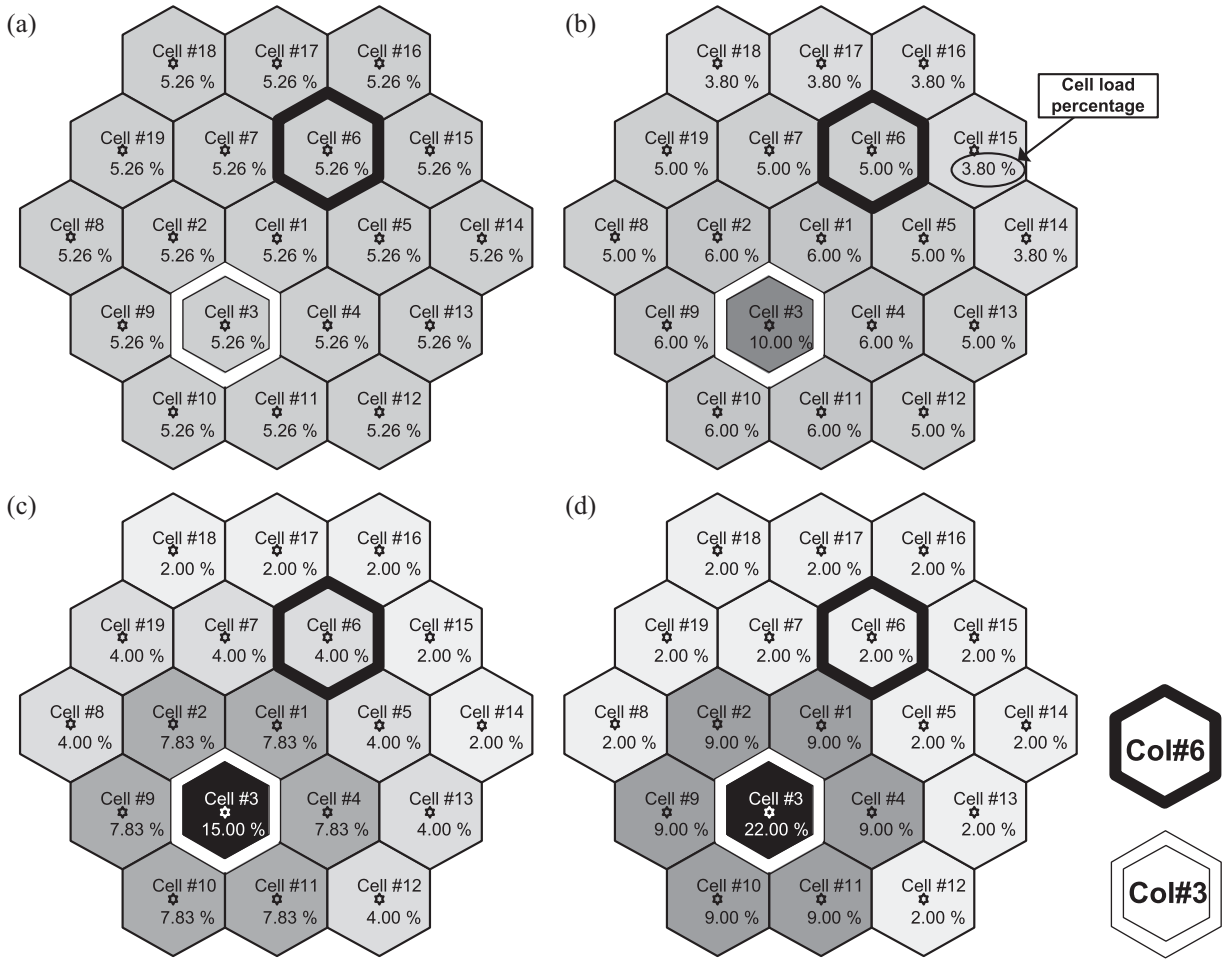


Fig. 5. Spatial load distribution for the four scenarios considered.

and (c) depict intermediate situations. For each scenario, the load percentage per cell and the cell number is included in the figure. Moreover, two Cells-of-Interest (CoI) are highlighted for the results in Section 6. CoI#3 represents the most loaded cell in the heterogeneous scenarios. On the other hand, CoI#6 represents a cell whose load percentage decreases throughout the patterns as load concentrates in CoI#3.

6. Results

A global comparison between fixed (FRF1, FRF3, PR, and SR) and dynamic (DSA1, DSA2, DSA3, DSA4) strategies has been performed. Fairness in the comparison is provided by setting the same system bandwidth for all the schemes. Nevertheless, it is worth mentioning that the same system deployments in terms

of cell radius and powers per chunk have been used for the following groups of schemes (a) DSA1, DSA2, FRF1, and FRF3, (b) DSA3 and PR, and (c) DSA4 and SR respectively.

Results shown here are given in terms of spectral efficiency, users' dissatisfaction probability and spectrum releasing capabilities according to the following definitions

The spectral efficiency per cell η is calculated as

$$\eta = \frac{\text{Total cell throughput}}{\text{Cell Bandwidth}} \text{ bits/s/Hz/cell.} \quad (10)$$

The average dissatisfaction probability $P^{T_{th}}$ is formally defined as

$$P^{T_{th}} = \frac{1}{\Gamma} \frac{1}{U} \sum_{t=1}^{\Gamma} \sum_{m \in U} \theta_m^{T_{th}}(t) \quad (11)$$

T_{th} is the user satisfaction throughput, Γ is the total number of frames in the observation period, U is the total number of users, and $\theta_m^{T_{th}}(t)$ is a satisfaction indicator per the m th user and the t th frame defined as $\theta_m^{T_{th}}(t) = \begin{cases} 1 & \text{th}_m(t) < T_{th} \\ 0 & \text{th}_m(t) \geq T_{th} \end{cases}$, where $\text{th}_m(t)$ is the average throughput that user m experiments during the last second before frame t .

Finally, to measure the capability of releasing spectrum in a given band for secondary cognitive radio usage the new metric called Useful Released Surface (URS) presented in Reference [20] is retained. The URS defines the surface where a given bandwidth can be used by secondary cognitive radio users respecting primary users' maximum interference level constrains. Formally, URS is defined as

$$URS = \sum_{n=1}^N B^{(n)} \sum_{a=1}^{\Lambda_n} S_a^{(n)} \omega_a^{(n)} \text{ MHz} \times \text{km}^2 \quad (12)$$

where $B^{(n)}$ is the bandwidth of the n th chunk and Λ_n is the set of non-contiguous areas where chunk n can be released. $S_a^{(n)}$ is the surface of each one of the areas, which is computed as the surface of all contiguous cells that do not use chunk n minus the surface of a protection area around cells that do use the n th chunk to protect from the interference primary users in them. Notice that with this definition, only the areas where secondary users are allowed to use the spectrum without harming primary users' transmissions are considered. Here the first tier of neighboring cells around a cell has been taken as a protection area. Finally, $\omega_a^{(n)}$ is a weighting factor for each area depending on the number of secondary cognitive radio users that exist on that area.

6.1. System Average Results

Figure 6 shows a global comparison between the algorithms studied here. Presented results come out

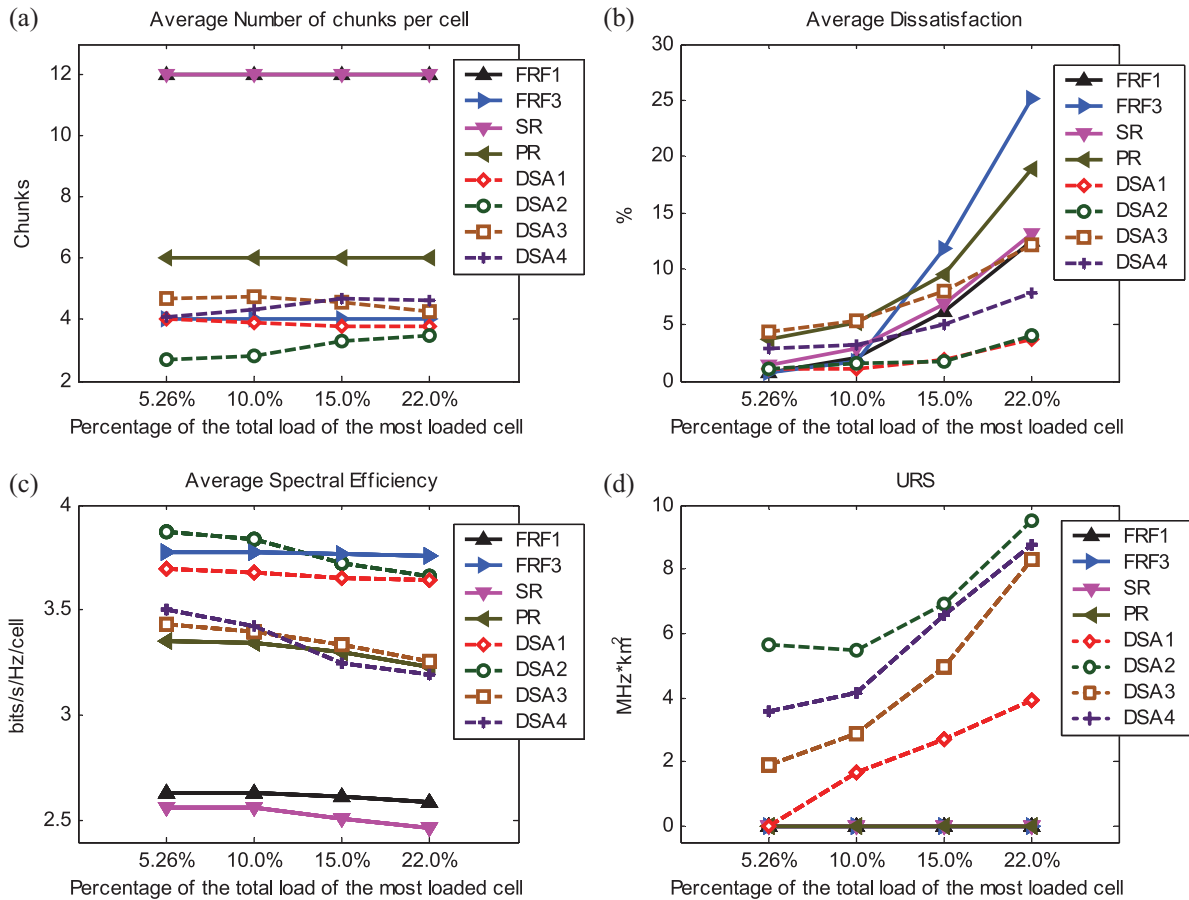


Fig. 6. Global system results.

from averaging all the partial results in each cell of the scenario. The average number of chunks deployed over the scenario is depicted in Figure 6(a). FRF1, PR, SR, and FRF3 schemes manifest no variation in the number of chunks assigned to each cell (12, 6, 12, and 4 chunks respectively out of $N = 12$ chunks available in the system). The average number of chunks per cell for the DSA algorithms is considerably reduced with respect to FRF1 or SR and remains around 4 chunks per cell. DSA2 algorithm exhibits the lowest values because of its better adaptability to the system's requirements by estimating the chunk capacity (contrary to DSA1 that maintains the chunk assignment regardless the real chunk capacity).

Dissatisfaction probability is depicted on Figure 6(b). For the homogeneous scenario (most loaded cell percentage equals to 5.26%) all DSA algorithms maintain dissatisfaction below target $P_{up} = 5\%$. In highly heterogeneous scenarios, DSA1, DSA2, and DSA4 demonstrate up to a 5% of absolute dissatisfaction reduction with respect to the best fixed reuse factor. DSA3 shows the highest dissatisfaction of the DSA algorithms but it remains below PR (up to 12% of absolute dissatisfaction reduction). Thus, DSA approaches maintain and even decrease dissatisfaction probability with respect to the fixed spectrum management schemes.

Average spectral efficiency is represented in Figure 6(c). DSA algorithms outperform the fixed schemes with the exception of FRF3 for highly heterogeneous scenarios. However, FRF3 as shown in Figure 6(b), presents the worst users' dissatisfaction for those scenarios. Focusing on the dynamic schemes, DSA2 ameliorates in spectral efficiency to DSA1 due to its precise adaptation to small variations of the chunk capacity conditions. Both algorithms improve at least 33% of the spectral efficiency with respect to FRF1 and SR. On the other hand, both DSA3 and DSA4 algorithms demonstrate slightly poorer spectral efficiency than the other DSA algorithms because the minimum number of chunks per cell is two (one for central and another for edge subband) instead of one as it is in the DSA algorithms. Thus, for low loaded cells, DSA3 and DSA4 algorithms assign more chunks than the minimum required and, as a result, the intercell interference increases, avoiding reaching high spectral efficiency. In any case, DSA3 and DSA4 performance is better than PR and SR respectively.

Finally, the Useful Released Area (URS) results are depicted on Figure 6(d). The first tier of cells has been taken as the protection area of primary users

(i.e., if a cell is using a chunk, secondary cognitive users cannot use this chunk in the neighboring cells, even if the chunk is free in those cells). Also, the area weighting factor $\omega_a^{(n)}$ is the fraction potential secondary users that would exist in an area assuming that they are uniformly distributed in the scenario. With this definition, the minimum URS value is one chunk free over a cluster of seven contiguous cells (i.e., $1.70 \text{ MHz} \times \text{km}^2$ for data in Table II). Contrary to the fixed reuse schemes, DSA algorithms evidence that it is possible to release spectrum in regional areas. It can be observed on Figure 6(d) that the URS increases as the users concentrate on a single cell (up to $9 \text{ MHz} \times \text{km}^2$ for DSA4). For the homogeneous case, it is impossible for DSA1 to release the spectrum with respect to the protection area. However, the rest of the DSA algorithms, by adapting the number of chunks taking into account realistic chunk capacities, enable the spectrum pooling and thus generate opportunities for secondary users. The DSA4 scheme is the best one in terms of URS performance overcoming all the other algorithms presented for all the cell loads examined.

Therefore, Figure 6 proves that DSA approaches improve in practice all the QoS metrics of the primary operator and, in particular, enable the creation of the secondary spectrum access opportunities into the licensed band, thus opening new business opportunities for the primary operator.

Finally, DSA1 and especially DSA2 show better performance than DSA3 and DSA4. This reflects that the dynamic approaches perform better as the freedom in assigning the chunks into the system band increases. In fact, the division between central and edge subbands incurs a limitation in a way that the chunks are assigned to cells. However, if the network operator decides to deploy PR or SR schemes to control the intercell interference, then it could actually switch to DSA3 or DSA4 that shows better performance than PR or SR respectively.

6.2. Cell and User Specific Results

Results in the previous section are averaged for all cells of the scenario and all users in the cells. However, some extra features of the DSA algorithms appear when metrics are observed for each individual cell. Specifically, cells of interest #3 and #6 highlighted on Figure 5 were under study.

Figures 7 and 8 depict individual cell results for CoI#3 and CoI#6 respectively. The average

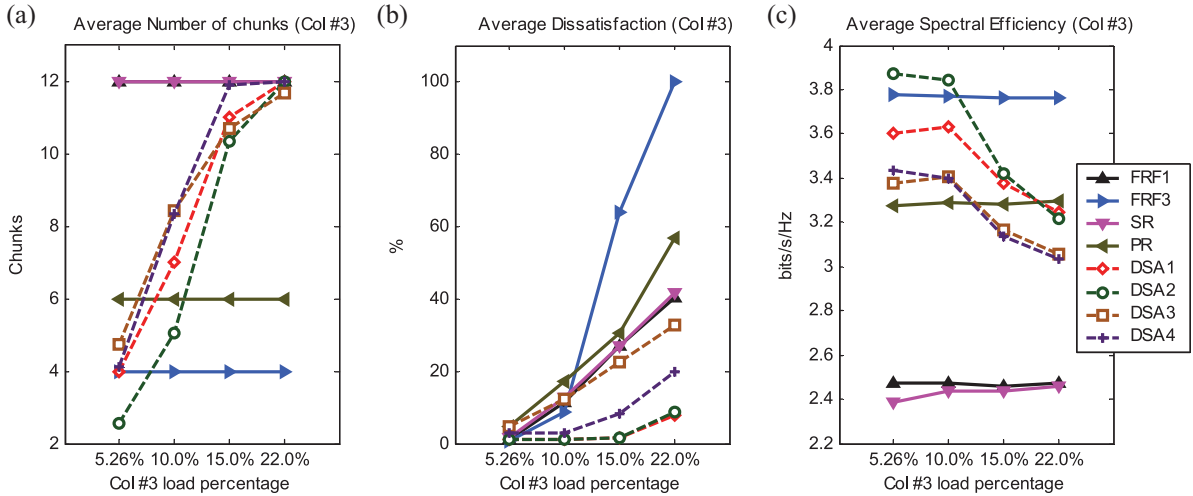


Fig. 7. Specific results for the most loaded cell (Col#3).

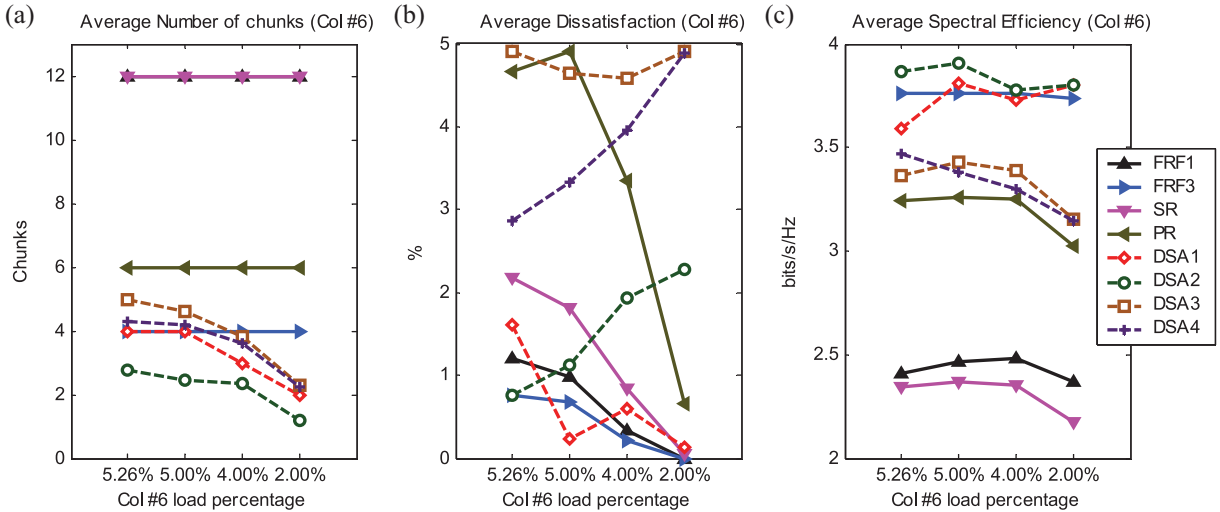


Fig. 8. Specific results for a cell decreasing its load (Col#6).

number of chunks assigned to Col#3 by DSA algorithms (Figure 7(a)) increases with the increase in the cell load until reaching the maximum number of available chunks. Col#3 manifests similar dissatisfaction probability behavior as the global system, since Col#3 is the dominant cell in the scenario. Spectral efficiency in this cell falls below 2.5 bits/s/Hz for high load (Figure 7(c)) because cells around it in Figure 5 also increase their load, their number of chunks, and thus the intercell interference (Col#3 uses almost all the chunks of the system for high loads).

On the other hand, the average number of chunks assigned to Col#6 decreases at the same

measure the cell load does (Figure 8(a)). For Col#6 the user's dissatisfaction maintains below $P_{up} = 5\%$ (Figure 8(b)) as expected. DSA2, DSA3, and DSA4 algorithms slightly increase the dissatisfaction in low loaded cells in order to achieve better spectral efficiency (Figure 8(c)) than FRF3 or FRF1, PR, and SR respectively. Therefore, DSA algorithms adapt spectrum usage on a cell-by-cell basis and feature an adequate trade-off between spectral efficiency and dissatisfaction probability.

Finally, in order to present the performance of the algorithms that introduce a band division between the central and edge subbands, Figure 9 depicts the dissatisfaction of edge users for PR, SR, DSA3, and

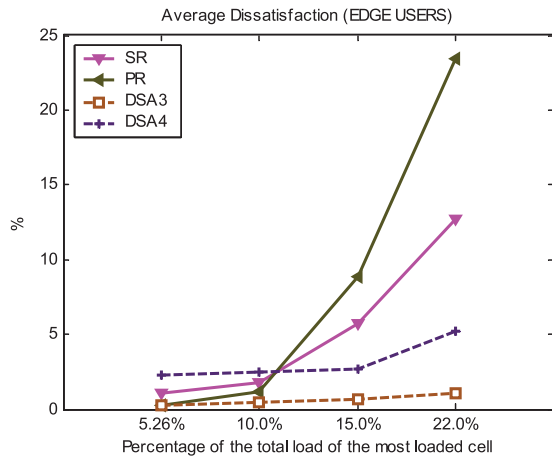


Fig. 9. Edge users' dissatisfaction.

DSA4 schemes. DSA3 and DSA4 obtain the best performance especially for high loads. Concretely around 20% of absolute dissatisfaction reduction is obtained for DSA3 with respect to PR in the most loaded case. Therefore, again, dynamic management of the spectrum regarding edge users improves their QoS.

7. Conclusions and Future Work

In this work, a set of novel DSA algorithms for multicell OFDMA scenarios has been proposed. It is claimed that the proposed framework can be very promising for future 4G wireless networks based on OFDMA technology since: (1) primary operator's spectral efficiency is improved, without degrading primary users' QoS and (2) new opportunities for secondary markets are created which open new business chances for spectrum holders and operators to obtain a profitable return from their investments in the expensive spectrum licenses. Hence, this framework can be a feasible solution to gradually evolve current networks and their spectrum regulatory rules in the context of e.g., the private commons paradigm.

Four DSA algorithms have been presented and tested over several scenarios with different spatial distributions of the traffic load, showing their capability to adapt the spectrum assignment to the different spatial and temporal traffic variations. These algorithms ameliorate the overall system's spectral efficiency at least 33% with respect to the total reuse of the frequency resources in the cellular system. At the same time, the DSA algorithms maintain or improve the satisfaction probability metric introduced in this paper up to 20% for users at the edge of the cell.

Thus, DSA algorithms show the best trade-off between spectral efficiency and satisfaction probability. It has also been demonstrated that the proposed DSA algorithms enable the releasing of the spectrum bands in large geographical areas so that this spectrum can be exploited by secondary cognitive radio users. This property has been assessed under several spatial load distributions including the homogeneous case, although the best performance is obtained under highly heterogeneous spatial distributions. Finally, it has been shown that the greater the freedom that the DSA algorithms have to perform the chunk-cell assignment, the better the performance obtained. Thus, DSA1 and especially DSA2, which benefit from more flexibility in the chunk assignment, show better performance than DSA3 and DSA4, which include constraints in the chunks to be assigned to the edge or central users. In any case, all the four considered strategies overcome the performance of classical PR and SR strategies.

In order to improve the proposed framework, the assessment of techniques such as meta-heuristics or machine learning has been identified as future work. Furthermore, other analysis to quantify the effect of assumptions like perfect CSI or perfect synchronization is also planned to be carried out. Finally, the exploration of distributed approaches toward a self-organized network composed of intelligent base stations is also under study.

Acknowledgements

This work has been performed in the framework of the project E³, which has received research funding from the Community's Seventh Framework programme. Also, the Spanish Research Council and FEDER funds under COGNOS grant (ref. TEC2007-60985) have supported this work. This paper reflects only the authors' views and the Community is not liable for any use that may be made of the information contained therein. The contributions of colleagues from E³ consortium and the support of the Spanish Ministry of Science and Innovation via FPU grant AP20051165 are hereby acknowledged.

References

1. Hoffmeyer JA. Regulatory and standardization aspects of DSA technologies – global requirements and perspectives. *1st IEEE International Symposium on in New Frontiers in Dynamic Spectrum Access Networks (DySPAN)* 2005; 700–705. DOI: 10.1109/DYSPAN.2005.1542699

2. FCC Spectrum Policy Task Force. Report of the spectrum efficiency working group 2002; [online] < <http://www.fcc.gov/sptf/reports.html> >. [date of access] 06/01/2008
3. Akyildiz IF, Lee W-Y, Vuran MC, Mohanty S. Next generation/dynamic spectrum access/cognitive radio wireless networks: a survey. *Computer Networks* 2006; **50**(13): 2127–2159. DOI: 10.1016/j.comnet.2006.05.001
4. Zhao Q, Sadler BM. A survey of dynamic spectrum access: signal processing, networking, and regulatory policy. *IEEE Signal Processing Magazine* 2007; **24**(3): 79–89. DOI: 10.1109/MSp.2007.361604
5. Buddhikot MM. Understanding dynamic spectrum access: models, taxonomy and challenges. *2nd IEEE International Symposium on in New Frontiers in Dynamic Spectrum Access Networks (DySPAN)* 2007; 649–663. DOI: 10.1109/DYSPAN.2007.88
6. FCC. Promoting efficient use of spectrum through elimination of barriers to the development of secondary markets. *Second Report and Order on Reconsideration and Second Further Notice of Proposed Rule Making*, 2004; [online] < http://wireless.fcc.gov/licensing/index.htm?job=secondary_markets >. date of access [6 January 2008].
7. Astély D, Dahlman E, Frenger P *et al.* A future radio-access framework. *IEEE Journal on Selected Areas on Communications* 2006; **24**(3): 693–706. DOI: 10.1109/JSAC.2005.862420
8. Wu Z, Nassar CR, Natarajan B, Wiegandt D. The road to 4g: two paradigm shifts, one enabling technology. *1st IEEE International Symposium on in New Frontiers in Dynamic Spectrum Access Networks (DySPAN)* 2005; 688–694. DOI: 10.1109/DYSPAN.2005.1542697
9. Weiss TA, Jondral FK. Spectrum pooling: an innovative strategy for the enhancement of spectrum efficiency. *IEEE Communications Magazine* 2004; **42**(3): 8–14. DOI: 10.1109/MCOM.2004.127376
10. Le B, Rondeau TW, Bostian CW. Cognitive radio realities. *Wireless Communications and Mobile Computing* 2007; **7**(9): 1037–1048. DOI: 10.1002/wcm.479
11. Prehofer C, Bettstetter C. Self-organization in communication networks: principles and design paradigms. *IEEE Communications Magazine* 2005; **43**(7): 78–85. DOI: 10.1109/MCOM.2005.1470824
12. Brito J. The Spectrum Commons in Theory and Practice 2007; [online] < <http://stlr.stanford.edu/pdf/brito-commons.pdf> >. date of access [6 January 2008].
13. 3GPP. TR 25.814. Physical layer aspects for evolved Universal Terrestrial Radio Access (UTRA), 2006; v7.1.0.
14. Li G, Liu H. Downlink radio resource allocation for multicell OFDMA system. *IEEE Transactions on Wireless Communications* 2006; **5**: 3451–3459. DOI: 10.1109/TWC.2006.256968
15. Jang J, Lee KB. Transmit power adaptation for multiuser OFDM systems. *IEEE Journal on Selected Areas on Communications* 2003; **21**(2): 171–178. DOI: 10.1109/JSAC.2002.807348
16. Wengertner JO, von Elbwart AGE. Fairness and throughput analysis for generalized proportional fair frequency scheduling in OFDMA. *61st IEEE Vehicular Technology Conference* 2005; Spring; **3**: 1903–1907. DOI: 10.1109/VETECS.2005.1543653
17. Sternad M, Ottosson T, Ahlen A, Svensson A. Attaining both coverage and high spectral efficiency with adaptive OFDM downlinks. *IEEE Vehicular Technology Conference* 2003; Fall.
18. Huawei TR1-050507. Soft Frequency Reuse Scheme for UTRAN LTE, *3GPP TSG RAN WG1* 2005.
19. Bernardo F, Pérez-Romero J, Sallent O, Agustí R. Advanced spectrum management in multicell OFDMA networks enabling cognitive radio usage, *IEEE Wireless Communications and Networking Conference (WCNC)* 2008; DOI: 10.1109/WCNC.2007.343

20. Nasreddine J, Pérez-Romero J, Sallent O, Agustí R. A primary spectrum management solution facilitating secondary usage exploitation. *17th ICT Mobile and Wireless Communications Summit* 2008.

Authors' Biographies



Francisco Bernardo received the Telecommunications Engineering degree at the ETSIT of the Universidad de Málaga (UMA), Spain, in 2004. He joined the Radio Communications Research Group of the Universitat Politècnica de Catalunya (UPC) in 2005 where he currently is a Ph.D. student. His research interests are in the field of wireless communications especially OFDMA wireless networks, dynamic spectrum management and cognitive radio. He has been involved in projects of the 6th and 7th Framework Programme of the European Commission. Currently he has a FPU grant of the Spanish Ministry of Education.



Ramón Agustí received the Engineer of Telecommunications degree from the Universidad Politécnica de Madrid, Spain, in 1973, and the Ph.D. degree from the Universitat Politècnica de Catalunya (UPC), Spain, 1978. In 1973 he joined the Escola Tècnica Superior d'Enginyers de Telecomunicació de Barcelona, Spain, where he became Full Professor in 1987. After graduation he was working in the field of digital communications with particular emphasis on transmission and development aspects in fixed digital radio, both radio relay and mobile communications. For the last 15 years he has been mainly concerned with the performance analysis, development of planning tools and equipment for mobile communication systems and he has published about 200 papers in those areas. He participated in the European program COST 231 and in the COST 259 as a Spanish representative delegate. He has also participated in the RACE and ACTS European research programs and currently in the IST as well as in many private and public funded projects. He received the Catalonia Engineer of the year prize in 1998 and the Narcis Monturiol Medal issued by the Government of Catalonia in 2002 for his research contributions to the mobile communications field. He is part of the editorial board of several Scientific International Journals and since 1995 is conducting a post graduate annual course on mobile communications. He has co-authored two books on Mobile communications.



Jordi Pérez-Romero is currently an associate professor at the Dept. of Signal Theory and Communications of the Universitat Politècnica de Catalunya (UPC) in Barcelona, Spain. He received the Telecommunications Engineering degree and the Ph.D. from the same university in 1997 and 2001. His research interests are in the field of mobile

communication systems, especially packet radio techniques, radio resource and QoS management, heterogeneous wireless networks, and cognitive networks. He has been involved in different European Projects as well as in projects for private companies. He has published papers in international journals and conferences and has co-authored one book on mobile communications.



Oriol Sallent is an associate professor at the Universitat Politècnica de Catalunya. His research interests are in the field of mobile communication systems, especially radio resource and spectrum management for heterogeneous networks. He has published more than 70 papers in international journals and conferences. He has participated in

several research projects of the 5th and 6th Framework Programme of the European Commission and served as a consultant for a number of private companies.